URSI GASS 2026, Krakow, Poland, 15 – 22 August 2026

Synchronization in LEO 5G-NTN: Challenges and Solutions

E. Mozo[(1)]*, M. Caus[(1)], A. Giuliani[(1)], P. Henarejos[(1)], P. Gawlowicz[(2)], J. Tallon[(2)] and M. Á. Vázquez[(1)]
(1) *Centre Tecnològic de Telecomunicacions de Catalunya (CTTC)*
(2) *Software Radio Systems (SRS)*

Abstract

Integrating Low Earth Orbit (LEO) satellites into 5G New Radio non-terrestrial networks (NR-NTN) poses stringent time–frequency synchronization requirements due to large Doppler shifts, fast Doppler dynamics, and time-varying propagation delays. These impairments impact downlink acquisition, uplink alignment, and ultimately link robustness. This paper characterizes the dominant synchronization bottlenecks in LEO NR-NTN and discusses practical mitigation techniques aligned with 3GPP Release 17 procedures and constraints. Experimental results obtained with a satellite channel emulator and software-defined radio modems show bounded residual carrier-frequency offset and stable timing behavior during an emulated LEO overpass. In particular, the uplink frame alignment error remains within 1 μs throughout the pass.

1 Introduction

The integration of non-terrestrial networks (NTN) into 5G New Radio (5G-NR) is a key enabler for ubiquitous connectivity beyond terrestrial coverage, including remote, rural, maritime, and airborne scenarios. Among NTN architectures, Low Earth Orbit (LEO) constellations are attractive due to their comparatively low latency, high spatial reuse, and global service potential [1]. However, extending NR to LEO satellite links introduces non-negligible physical-layer impairments. Time–frequency synchronization becomes particularly critical because the high orbital velocity of LEO satellites yields large Doppler shifts and Doppler rates, while long and time-varying slant ranges produce substantial propagation delays and delay dynamics. These effects directly challenge core receiver operations, including synchronization signal block (SSB) detection, carrier frequency offset (CFO) estimation, and timing acquisition.

Terrestrial NR synchronization procedures are typically designed under limited Doppler and slowly varying delay assumptions, which can be violated in LEO NTN. Depending on carrier frequency and elevation, Doppler shifts may reach several tens of kilohertz, potentially exceeding the acquisition range of baseline synchronization algorithms. In addition, residual timing errors and delay dynamics may lead to cyclic prefix (CP) violations and inter-symbol interference (ISI), degrading both initial access and data-phase performance.

Recent work has explored satellite-oriented synchronization enhancements [2, 3], including ephemeris-assisted Doppler pre-compensation, improved frequency tracking, and refined timing estimation. For instance, [4] proposes Doppler mitigation at base station side to sustain continuous communication in LEO NR-NTN, being this approach not standard-compliant. However, a consolidated assessment of synchronization bottlenecks together with practical solutions that remain compatible with NR procedures and constraints is still needed. Accordingly, this paper discusses and evaluates time–frequency synchronization strategies that mitigate LEO-induced impairments while adhering to practical NR-NTN implementation constraints.

Contributions and scope: The main contributions of this work are threefold. First, we provide a compact yet quantitative characterization of the dominant time–frequency impairments in LEO NR-NTN initial access and tracking, emphasizing the joint impact of Doppler shift, Doppler rate, and delay dynamics on OFDM-based acquisition. Second, we describe practical synchronization adaptations that fit within NR-NTN procedures and constraints, including an extended PSS detector with an explicit CFO-hypothesis bank and an uplink timing strategy that combines System Information Block (SIB) 19 assistance with sample-level buffering to track delay variations across the pass. Third, we validate these mechanisms in an software-define radio (SDR) based testbed with an emulated *BlueWalker 3* overpass, reporting residual CFO statistics and uplink alignment bounds at the Next Generation Node B (gNB) base station.

2 5G-NR NTN System Model

We consider a LEO satellite–based NR-NTN system aligned with 3GPP Release 17. The satellite acts as a spaceborne gNB and serves terrestrial user equipment (UE) over a wide footprint. The satellite follows a circular LEO orbit of altitude h and orbital velocity v_s, resulting in a time-varying relative motion with respect to the UE. For clarity, we distinguish three frequency terms that contribute to the effective CFO observed at the UE. Let $f_D^{DL}(t)$ denote the Doppler shift due to relative motion on the downlink carrier, and let f_{osc} represent the (approximately constant over minutes) oscillator-induced mismatch between the satellite payload and the UE reference. Then, the aggregate downlink CFO is

$$\Delta f^{DL}(t) = f_D^{DL}(t) + f_{\text{osc}}. \quad (1)$$

Similarly, on the uplink, the Doppler term differs due to the UL carrier frequency, resulting in

$$\Delta f^{UL}(t) = f_D^{UL}(t) + f_{\text{osc}}. \tag{2}$$

While f_{osc} is slowly varying, $f_D^{DL}(t)$ and $f_D^{UL}(t)$ vary with satellite geometry and can change noticeably within a short interval, motivating both frequency tracking and pre-compensation.

In addition to the delay $\tau(t)$, its time derivative $\dot{\tau}(t)$ is relevant because it induces timing drift across frames. In OFDM, residual timing error beyond the CP can cause ISI, whereas residual CFO causes inter-carrier interference (ICI). Hence, the objective of the proposed synchronization chain is to maintain residual timing within the CP margin and residual CFO within a range that ensures negligible ICI under the considered numerology.

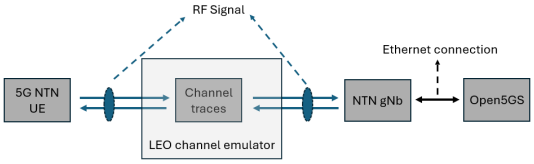

Figure 1. LEO NR-NTN system emulation framework.

The considered model is implemented in an experimental framework combining a satellite channel emulator, two SDR-based modems, and a workstation hosting the core network, as shown in Fig. 1. Channel traces are generated from a two-line element (TLE) description of the *BlueWalker 3* satellite for a five-minute visibility window. These traces are synchronized with the SIB 19 information broadcast by the gNB. Each modem implements either UE or gNB functionality using a USRP platform and a workstation. The NR-NTN waveform occupies 5 MHz bandwidth with 15 kHz subcarrier spacing.

3 Synchronization Challenges

Time–frequency synchronization in LEO NR-NTN is more demanding than in terrestrial NR primarily due to (i) large Doppler shifts and Doppler rates and (ii) large and time-varying propagation delays. These impairments affect both DL acquisition/tracking and UL alignment.

Doppler shift and Doppler rate: LEO orbital velocity can produce Doppler shifts f_D on the order of tens of kilohertz, depending on f_c and elevation. Such offsets may exceed the acquisition range of baseline NR synchronization, degrading CFO estimation and potentially hindering SSB detection. For *BlueWalker 3* at $h \approx 491$ km and $f_c = 1.7$ GHz, Doppler values up to approximately ± 40 kHz may be observed. In OFDM, large uncompensated Doppler also induces ICI, reducing subcarrier orthogonality. Moreover, the Doppler rate introduces intra-frame frequency variation, limiting the effectiveness of quasi-static frequency compensation and increasing residual frequency error.

Propagation delay and timing uncertainty: The satellite slant range results in propagation delays that are orders of magnitude larger than in terrestrial links and vary over time. While terrestrial NR timing assumptions are typically compatible with small round-trip-time (RTT) values, LEO RTTs may span several milliseconds. For *BlueWalker 3*, a representative RTT range is 1.6–8 ms. This timing uncertainty complicates frame and symbol alignment, particularly during initial access and UL timing. Uncompensated timing errors can cause CP violations and ISI; conversely, enlarging timing search windows increases complexity and latency. Hence, LEO NR-NTN generally requires NTN-specific adaptations for robust synchronization.

Impact on OFDM acquisition and demodulation: In NR, the tolerable residual CFO depends on subcarrier spacing (SCS) and receiver tracking. A large initial CFO can severely attenuate correlation peaks used for synchronization sequences and can smear the timing metric, especially under Doppler rate. Moreover, ICI power increases with the normalized offset $|\Delta f|/\text{SCS}$, so bounding residual CFO after coarse acquisition is essential to preserve demodulation performance. On the timing side, the delay variation across an overpass can translate into a non-negligible drift across slots if left uncompensated. Since NR assumes timing alignment within a bounded window (with additional NTN-specific assistance), the receiver must handle both a potentially large absolute delay and its variation. This motivates (i) reducing the initial timing uncertainty using broadcast assistance and (ii) applying tracking to counteract the time-varying component, so that the residual timing error stays within the CP margin during data transmission.

4 Proposed Synchronization Solutions

This section presents practical DL and UL synchronization solutions for NR-NTN [5]. The implementations are based on the srsRAN project [6].

4.1 Downlink Synchronization

DL synchronization relies on successful SSB detection to acquire coarse timing and frequency. To enhance robustness under large CFO uncertainty, we employ an NTN-oriented PSS detector with $2N+1$ parallel correlation branches, enabling a joint search in time and frequency. Each branch is matched to a CFO hypothesis $m_k = k\Delta f$, where Δf denotes the hypothesis spacing and $-N \le k \le N$. As CFO uncertainty grows with the maximum perceived Doppler, N must be increased accordingly. The UE selects the branch yielding the largest correlation peak ρ_k, providing a coarse estimate of timing and frequency offsets.

The hypothesis spacing Δf is selected as a trade-off between acquisition robustness and computational cost. A

smaller Δf reduces quantization error in the coarse CFO estimate but increases the number of correlators $2N+1$ needed to span the uncertainty range. In practice, N is chosen to cover the worst-case Doppler plus an additional margin for oscillator mismatch, i.e.,

$$N \geq \left\lceil \frac{f_{\max}}{\Delta f} \right\rceil, \quad f_{\max} \approx |f_D|_{\max} + |f_{\text{osc}}|_{\max}. \tag{3}$$

The resulting detector cost scales linearly with the number of branches, and the implementation exploits pre-rotations of the received samples per hypothesis to reuse the same correlator kernel. This keeps the approach practical for real-time SDR execution while extending the acquisition range beyond baseline terrestrial assumptions.

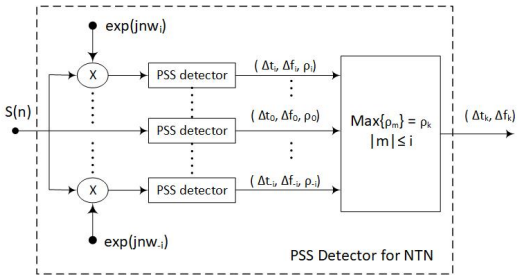

Figure 2. NTN PSS detection via parallel CFO hypotheses.

Figure 2 illustrates the approach: from the received signal, the timing offset Δt_k and coarse frequency offset Δf_k are jointly obtained. These estimates are used to compensate the incoming signal prior to PBCH decoding. Subsequently, Δf_k is refined using residual CFO measurements derived from broadcast-channel processing. Conceptually, Δf_k aggregates (i) Doppler-related frequency shift and (ii) oscillator-induced CFO due to transponder and modem frequency references.

4.2 Uplink Synchronization

After DL synchronization, the UE performs uplink synchronization through the random access (RA) procedure (four-step exchange). To reduce UL timing misalignment under large and time-varying RTT, we adopt a modified RA behavior in which the UE applies a sample-level timing advance

$$TA_{\text{UE}}[n'] = RTT[n'] - \left\lfloor \frac{RTT[n']}{I_t} \right\rfloor I_t \tag{4}$$

derived from SIB 19 assistance information, as illustrated in Fig. 3. Where $\lfloor \cdot \rfloor$ is the integer part, n' indexes SIB 19 updates, and I_t is the transmission time interval (TTI).

Applying TA_{UE} prior to Msg1 aims to keep the received preamble within the CP duration at the gNB. Since RTT evolves during the pass, UL timing must be tracked after RA. We implement a time-varying digital buffer that delays UL complex samples by $t_b[i]$ prior to transmission; the mechanism is summarized in Algorithm 1. Let pos_{ue} and pos_{sat} be the UE and satellite position vector, respectively.

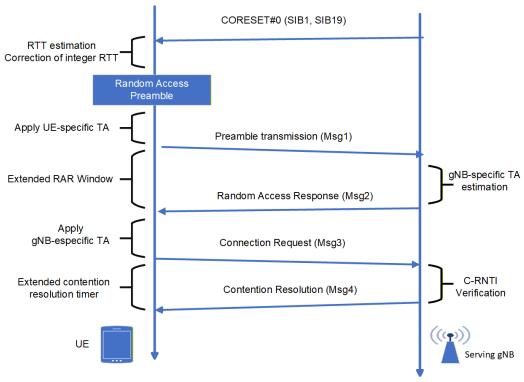

Figure 3. Random access procedure adapted for NTN.

Algorithm 1 Uplink tracking algorithm

1: **while** True **do**
2: Read SIB 19 from the serving cell
3: Derive $RTT[n']$ from $pos_{ue}[n']$ and $pos_{sat}[n']$
4: Compute $TA_{\text{UE}}[n']$ using (4)
5: Estimate $RTT[i]$ at each i-th TTI via interpolation
6: Set buffer delay $t_b[i] = k_{\text{offset}} - RTT[i]$
7: Apply buffer to subsequent UL transmissions
8: **end while**

Finally, UL frequency pre-compensation is applied. For each i-th TTI, the UL pre-compensation term is given by

$$\Delta f_k^*[i] = (\Delta f_k[i] - f_D^{DL}[i])\, F_c - f_D^{UL}[i], \tag{5}$$

where $f_D^{DL}[i]$ and $f_D^{UL}[i]$ denote DL and UL Doppler values derived from SIB 19 as per [7], and F_c is the UL/DL carrier-frequency ratio. The term $\Delta f_{\text{osc}}[i] = \Delta f_k[i] - f_D^{DL}[i]$ provides a coarse estimate of oscillator-induced CFO.

5 Performance Evaluation

We evaluate the proposed procedures using the LEO NR-NTN framework of Section 2. Figure 4 reports frequency-related metrics estimated by the UE from SIB 19 assistance information and DL measurements. As expected, the Doppler-related component changes sign near the midpoint of the pass and spans approximately ± 40 kHz over the visibility window. The estimated $\Delta f_k^*[i]$ is used to pre-

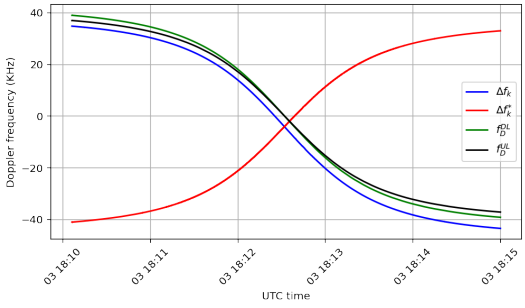

Figure 4. Frequency metrics computed by the UE.

compensate UL transmissions to improve frequency align-

ment at the gNB, whereas $\Delta f_k[i]$ is used for DL compensation at the UE. In addition, the inferred component Δf_{osc} remains almost constant around 4.2 kHz over the pass.

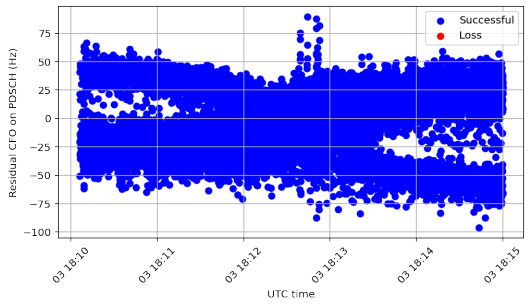

Figure 5. Residual CFO measured on PDSCH.

To quantify downlink frequency-tracking performance, we compute the residual CFO Δf_r on the physical downlink shared channel (PDSCH). Figure 5 shows that Δf_r is predominantly bounded within ± 75 Hz over the full pass, with a mean value of 0.48 Hz. No packet loss is observed at a transmission rate of 100 packets/s. Occasional excursions above 75 Hz are attributed to interpolation and update inaccuracies in the tracking of $f_k[i]$. In addition to the mean value, the residual CFO distribution remains concentrated: most samples fall well within the ± 75 Hz envelope, indicating stable tracking across the pass. This is consistent with the observation of zero packet loss at 100 packets/s under the considered configuration and suggests that the remaining frequency error is dominated by tracking-update granularity rather than by acquisition failures.

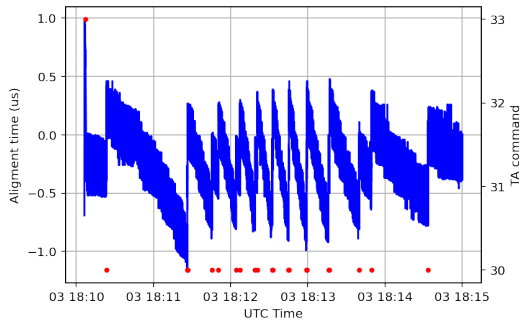

Figure 6. Uplink alignment error during PUSCH reception.

Finally, Fig. 6 shows the frame alignment error ε_r measured at the gNB during physical uplink shared channel (PUSCH) reception. When a misalignment is detected, the gNB transmits a timing advance (TA) command to compensate the observed error. The results show that ε_r remains within ± 1 μs in the pass. Only a limited number of TA commands are issued, with the initial one corresponding to the RA phase (Msg3). These results support the effectiveness of the proposed digital-buffer tracking for time-varying LEO delay, while also indicating that more advanced tracking could further reduce or eliminate TA updates.

The experimental results confirms that combining broadcast assistance (SIB 19) with receiver-side enhancements can keep residual CFO and timing misalignment tightly bounded during an emulated LEO pass. However, some limitations should be noted. First, the accuracy of timing and Doppler assistance depends on ephemeris precision and update periodicity; coarse updates require interpolation, which may introduce tracking errors. Second, although the uplink buffering strategy compensates delay variations at the sample level, it could be improved with a closed-loop estimator based on gNB feedback to reduce TA commands. Third, while this study focuses on synchronization stability, the same residual impairments can affect higher-layer mechanisms (e.g., HARQ timing, scheduling and retransmissions), requiring future cross-layer analysis.

6 Conclusion

This paper examined time–frequency synchronization in LEO NR-NTN under realistic overpass dynamics. The discussed synchronization procedures bound residual frequency error and maintain UL timing alignment across the visibility window, enabling stable DL/UL operation with a limited number of timing-advance updates. Future work will explore more sophisticated tracking methods to improve robustness under faster delay dynamics and to further reduce (or remove) the need for TA commands.

7 Acknowledgements

This work has been supported by the project 5G-STARDUST, which has received funding from the Smart Networks and Services Joint Undertaking of the European Union's Horizon Europe research and innovation programme under Grant Agreement No. 101096573.

References

[1] T. Darwish *et. al.*, "LEO Satellites in 5G and Beyond Networks: A Review From a Standardization Perspective," *IEEE Access*, March 2022.

[2] S. Kumar *et. al.*, "5G NTN LEO Based Demonstrator Using OpenAirInterface5G," *40th International Communications Satellite Systems Conference* , 2023.

[3] J. Zhu, Y. Sun, and M. Peng, "Timing Advance Estimation in Low Earth Orbit Satellite Networks," *IEEE Transactions on Vehicular Technology*, Oct. 2023.

[4] A. K. Meshram *et. al.*, "Doppler Effect Mitigation in LEO-Based 5G Non-Terrestrial Networks," *IEEE Globecom Workshops*, 2023.

[5] 3GPP TR 38.821 V16.2.0, "Solutions for NR to Support Non-Terrestrial Networks (NTN)," Apr. 2023.

[6] Software Radio Systems, "Open Source RAN," *https://www.srsran.com*.

[7] 3GPP TR 38.811 V15.1.0, "Study on New Radio (NR) to Support NTN," Jun. 2019.